ELSEVIER

Polymer 41 (2000) 8167–8171

polymer

www.elsevier.nl/locate/polymer

Polymer Communication

Surface adsorption layer of propylene on polyimide

T. Miyazaki*, A. Shimazu, K. Ikeda

Nitto Denko Corporation, 1-1-2, Shimohozumi, Ibaraki, Osaka 567-8680, Japan

Received 22 December 1999; received in revised form 6 March 2000; accepted 10 March 2000

Abstract

X-ray reflectivity measurements were performed on a polyimide thin film in propylene. The film was synthesized from 2,2-bis(3,4-carboxyphenyl)hexafluoropropane dianhydride (6FDA). In propylene at a relative vapor pressure $P/P_0 > 0.55$, an additive layer was detected on the polyimide surface. The layer thickness increased with the relative vapor pressure. At $P/P_0 = 0.96$, the layer thickness was about 6 nm. However, the thickness decreased rapidly with temperature. It was thought that the layer was composed of propylene. The propylene permeability increased substantially at $P/P_0 > 0.6$. The adsorbed layer was thought to play an important role in the increase in the propylene permeability.

Keywords: X-ray reflectivity; Polyimide; Propylene adsorption

1. Introduction

Polyimides with 2,2-bis(3,4-carboxyphenyl)hexafluoropropane dianhydride (6FDA) have been reported to exhibit good performance for the separation of olefin gases from paraffin gases compared with the other conventional polymers [1–4].

Recently, in the 1,3-butadiene/*n*-butane [5] and propylene/propane [6] separation systems, we found that some of the 6FDA-based polyimide films showed very high olefin permeability compared with paraffin gases. The ideal separation factor for 1,3-butadiene versus *n*-butane for the 6FDA-based polyimide synthesized from 2,2-bis (4-aminophenyl)-hexafluoropropane(BAAF) was about 20,000 at 25°C. Moreover, we found that the 1,3-butadiene diffusion coefficient was approximately 20,000 times greater than that of *n*-butane, even though the solubility of 1,3-butadiene was equivalent to that of *n*-butane [5]. However, the separation factor in the mixed gas system was about 3. The swelling of the film induced by 1,3-butadiene was then considered.

Therefore, we have investigated the swelling behavior of two kinds of 6FDA-based polyimides by 1,3-butadiene and *n*-butane using X-ray reflectivity measurements [7]. X-ray reflectivity measurements have generally been used for the measurement of the thickness of thin polymer films (~300 nm) [8,9]. The thickness determination accuracy is very high; the estimated error is within a few angstroms [8–13].

In Ref. [7], the thickness increase of the films by 1,3-butadiene and *n*-butane were observed at 0–2.3 atm. Up to 1.5 atm, the thickness increased linearly along almost the same line in both cases. Above that pressure, large expansions occurred upon the introduction of 1,3-butadiene. Finally, the film thickness increased by 30% in 1,3-butadiene at 2.3 atm ($P/P_0 = 0.83$) but only by 10% in *n*-butane at the same pressure ($P/P_0 = 0.96$). The 6FDA-based polyimide was significantly swollen by 1,3-butadiene compared with *n*-butane. Moreover, for one of the polyimides, a surface thin layer on the polyimide was detected in 1,3-butadiene at 2.3 atm.

We believed that the layer was composed of 1,3-butadiene. However, we could not characterize the film structure in detail because the thickness was only 3 nm. It is very important that the layer is confirmed to be an adsorption layer of 1,3-butadiene because a different permeation mechanism of hydrocarbon gases from that of non-organic gases like oxygen, nitrogen or carbon dioxide, which are considered as the ideal gases, may be required for the explanation of the hydrocarbon permeation phenomenon.

Recently, we found that the thickness of the surface layer in propylene was much larger than that in 1,3-butadiene. The thickness was about 6 nm at the relative vapor pressure $P/P_0 > 0.9$. The layer was detectable at $P/P_0 > 0.55$. We also detected a rapid increase in the peameability at $P/P_0 > 0.6$, which may be due to the surface adsorption of propylene.

* Corresponding author. Tel.: +81-726-21-0269; fax: +81-726-21-0307.

E-mail address: tsukasa_miyazaki@gg.nitto.co.jp (T. Miyazaki).

0032-3861/00/$ - see front matter
PII: S0032-3861(00)00189-0

6FDA-BAAF

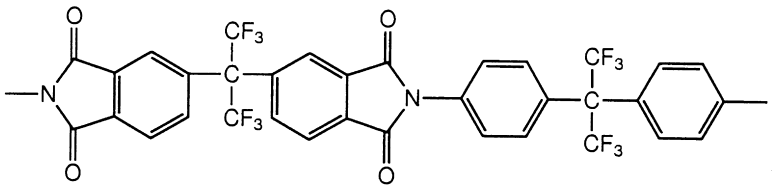

Fig. 1. Chemical structure of polyimide used in this study.

2. Experimental section

The chemical structure of the polyimide used in this study is shown in Fig. 1. The diamine used was 2,2-bis(4-aminophenyl)hexafluoropropane(BAAF). The polyimide used was prepared by chemical imidization methods in this laboratory. Refer to Ref. [5] for preparation of the polymer.

The permeability coefficients of propylene were measured by a pressure transform method with an applied pressure of relative vapor pressure of 0.13–0.85. For details, refer to Ref. [5].

Polyimide thin films for X-ray reflectivity measurements were prepared on Si(111) wafers. The 2.5% (6FDA-BAAF(1)) and 5% (6FDA-BAAF(2)) by weight polymer solution in diethylene glycol dimethyl ether was filtered (2 μm pore size) and spun cast at 2000 rpm on cleaned silicon wafers. Each sample was baked at 110°C for 1 h, then at 150°C for 3 h, and then air-dried at 190°C for 12 h to remove any residual solvent.

The index of refraction at X-ray energies is slightly less than one and is typically written as $n = 1 - \delta - i\beta$, where

$$\delta = \frac{r_e \lambda^2}{2\pi} \frac{\rho}{M} N_0 \sum_{i=1}^{n} x_i f_{1i} \quad (1)$$

$$\beta = \frac{r_e \lambda^2}{2\pi} \frac{\rho}{M} N_0 \sum_{i=1}^{n} x_i f_{2i} \quad (2)$$

Here, r_e is the classical electron radius, λ the X-ray wavelength, M the molecular weight, ρ the mass density, N_0 Avogadro's number, x_i the molar fraction of the ith atom of the atomic scattering factor f_i of the real and imaginary components, f_{1i} and f_{2i}, and n is the number of atoms in a molecule.

The reflection of X-rays from a layered medium was discussed by Parratt [14] who derived a recursion formula to calculate the reflected intensity from successive interfaces. The theory was later modified to include the effects of interface roughness [15].

The calculated model spectra using the recursion formula were converted to the X-ray reflectivity data by the non-linear least squares method. Each layer was described by four parameters: δ (in Eq. (1)), β (in Eq. (2)), thickness and roughness. However, it has been noted that the absorption effect is very small for polymer systems, so we assumed β to be constant. One additional parameter is a scale factor that is shifted for the overall data. Another parameter is an offset angle that is needed to convert the experimental θ into absolute θ (e.g. $\theta = 0$ corresponding to the sample parallel to the incident beam). The calculated reflectivity was convoluted with a Gaussian function representing the instrumental resolution function.

We used the following goodness-of-fit parameter

$$\chi^2 = \frac{1}{N-m} \sum_{n=1}^{N} \left(\frac{R_o - R_c}{R_o} \right)^2$$

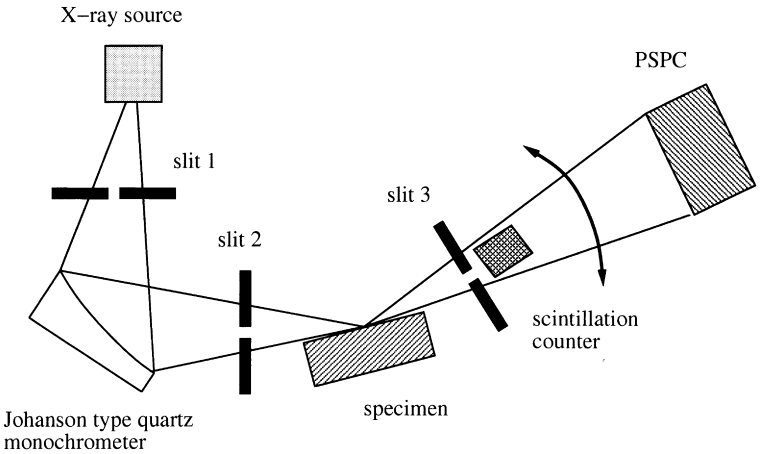

Fig. 2. Schematic diagram of the X-ray reflectometer.

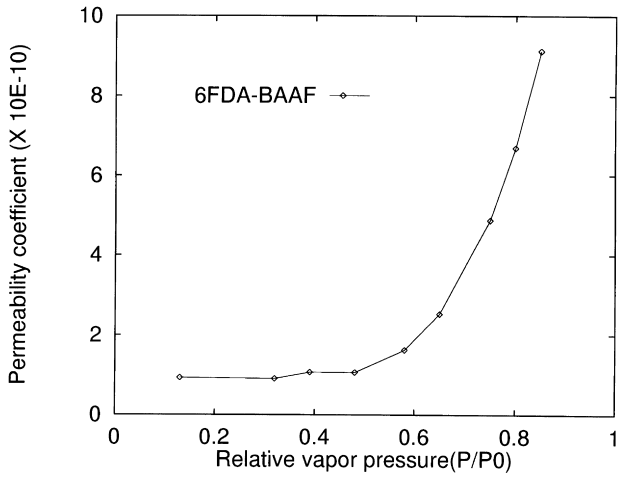

Fig. 3. Permeability coefficient (cm^3(STP)cm/cm^2 s cmHg) of propylene.

where R_o and R_c are the observed and calculated reflectivities, respectively, N the total number of data points, and m the number of fitting parameters.

The X-ray reflectivity experiments were performed using a two-circle goniometer based on a 2 kW standard X-ray tube. We developed this reflectometer newly for this study. A schematic drawing of the instrument is shown in Fig. 2.

The sample environment was maintained in a chamber with two beryllium windows under a vacuum or with propylene. The window thickness was 2 mm. The chamber was placed on the θ axis of the goniometer.

CuKα X-rays were selected by reflection from a Johanson type quartz monochrometer. The monochromatic beam was then focused on the sample. The measurements were performed in two modes. One of them is the counter scan mode, which is usually used. In Fig. 2, slit 1, slit 2, slit 3 and the scintillation counter mounted on the 2θ axis are used.

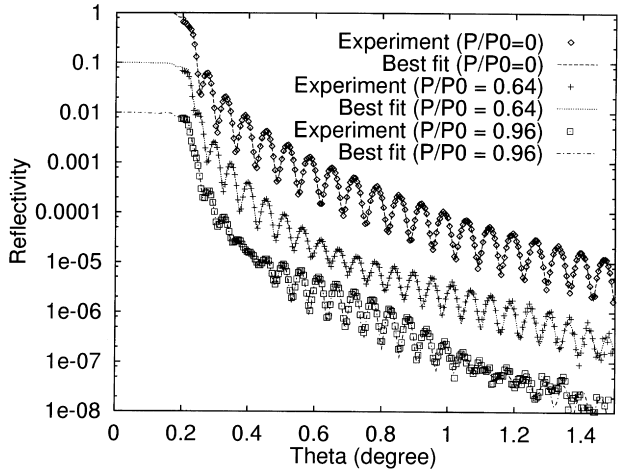

Fig. 4. X-ray reflectivities of 6FDA-BAAF(1) film in a vacuum (Experiment: ◇, Calculation: — —), in propylene at $P/P_0 = 0.64$ (Experiment: +, Calculation: - - -) and in propylene at $P/P_0 = 0.96$ (Experiment: □, Calculation: –·–·–·).

Slit widths are 0.05, 0.1 and 0.15 mm, respectively. A θ–2θ scan is taken to measure the specular reflection signal after completely aligning the sample.

The other mode is used for the rapid characterization of the structural change of thin film systems induced by the sample environment. We call this mode the "RC mode". None of the slits are used. For this arrangement, all X-rays strike the sample surface at a glancing angle within $\Delta\theta$, which is equal to the focusing angle. In spite of the scintillation counter, a one-dimensional position sensitive proportional counter (PSPC) located 1500 mm away from the sample is used. Without counter and sample scans, it simultaneously counts all X-rays reflected within $\Delta\theta$ from the sample surface. As the direct beam intensity for the counter scan mode is very weak (about 30000 counts/s), which is due to the large absorption by the two beryllium windows of 2 mm thickness, a typical measurement time in the counter scan mode is 23 h. However, a typical measurement time is 180 s in the RC mode. We will publish details elsewhere about our instrument and quantitative data corrections for the RC mode.

3. Results and discussion

Fig. 3 shows the dependency of the permeability coefficient of propylene on an applied pressure. A sudden increase in the permeability coefficient beyond the relative vapor pressure, $P/P_0 > 0.6$ was observed.

Figs. 4 and 5 show the X-ray reflectivity data for the as-deposited films under vacuum and in propylene at the relative vapor pressure shown in the figures. The most obvious effect of exposure to gas is an increase in the oscillation frequency corresponding to an increase in the film thickness. In propylene, the thickness of the 6FDA-BAAF film increased substantially compared with the as-deposited films. Good fits to the data could be obtained in the cases of the as-deposited films under vacuum using a model with only a single polyimide film on silicon. However, over $P/P_0 > 0.25$, the fits to the data became very poor using the same model. The observed data could be reproduced by the addition of a surface low density layer to the model. However, the best fits could not be obtained under $P/P_0 = 0.5$. This was most likely due to the thinness of the surface layer. It was thought that wider range measurements were required for the analysis of the surface layer of a thickness under 3 nm.

The fits of the data are shown by the dashed lines in the figures according to the parameters in Table 1 and 2. Good fits were obtained. The χ^2 values are 0.02–0.04 for 6FDA-BAAF(1) and 0.02–0.06 for 6FDA-BAAF(2). The thicknesses of the as-deposited film were 66.8 nm for 6FDA-BAAF(1) and 30.7 nm for 6FDA-BAAF(2). The density of the regular 6FDA-BAAF thick dense film is 1.47 g/cm^3. All film densities agreed with the density of their regular thick dense film.

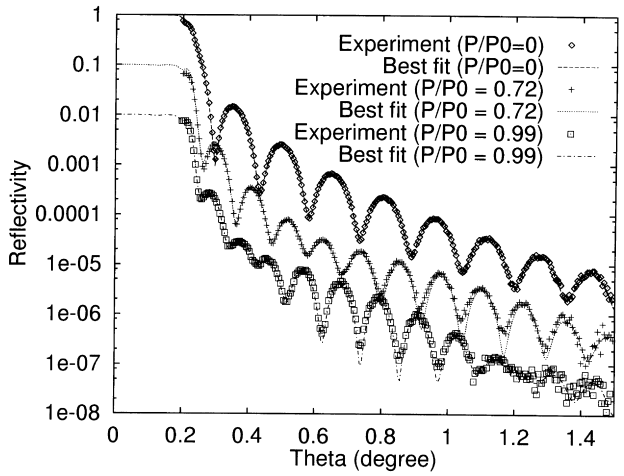

Fig. 5. X-ray reflectivities of 6FDA-BAAF(2) film in a vacuum (Experiment: ◇, Calculation: — —), in propylene at $P/P_0 = 0.72$ (Experiment: +, Calculation: - - -) and in propylene at $P/P_0 = 0.99$ (Experiment: □, Calculation: –·–·–·).

Moreover, in propylene, there are "nodes" in the oscillation as shown by Figs. 4 and 5. For example, in the case of 6FDA-BAAF(1)(Fig. 4), the position of the "node" is about $\theta = 0.6°$ at $P/P_0 = 0.64$ and $\theta = 0.4°$ at $P/P_0 = 0.96$, which is due to the surface low density layer. The higher the relative vapor pressure, the lower the position of the "node". This indicates an increase in the surface layer thickness with the relative vapor pressure. At $P/P_0 > 0.9$, the thickness was about 6 nm. This surface layer may be induced by the swelling or by the X-ray radiation. However, the measurements were repeated at the same relative vapor pressure, and good reproducibility was found. Moreover, the surface layer immediately disappeared when the sample chamber was placed under vacuum again.

Fig. 6 shows the dependency of the reflectivity data on temperature at a fixed propylene pressure ($P/P_0 = 0.96$ at 298 K) for 6FDA-BAAF(1). The "node" was shifted to a high angle, which indicated a decrease in the surface layer thickness. This "node" shift was also rapidly induced by a temperature change. Fig. 7 shows the raw reflectivity data for 6FDA-BAAF(2) at each temperature indicated in the figure for the RC mode. The channel number can be identified by the reflective angle. The measurement of each data took 3 min and the change in temperature took 1 min. The "node" located at the channel number of 280 at 299 K was rapidly shifted to a larger number by the temperature increase. One possible explanation for the observed phenomenon is that the surface layer consists of highly condensed propylene.

Many studies have been performed on the vapor adsorption layer of *n*-alkanes or other hydrocarbon gases on a solid at room temperature under saturated vapor pressure [16–24]. The formation of the vapor adsorption layer could be due to a van der Waals interaction with the solid. For example, Beaglehole et al. reported the vapor adsorption of *n*-pentane, cyclohexane, tetrachloromethane, octamethylcyclotetrasiloxane and water on mica and silicone [24]. They measured the adsorption isotherms on silicone and mica by ellipsometry as a function of P/P_0. They found an adsorption layer with a thickness of about several few nanometers on silicone over $P/P_0 = 0.9$ except for water. The thickness of the adsorption layers is consistent with that of our surface layers on the polyimide.

The increase in the 6FDA-BAAF film thickness was about 30% in 1,3-butadiene at $P/P_0 = 0.83$, while it was about 10% in *n*-butane at $P/P_0 = 0.96$ [7]. In propylene, the 6FDA-BAAF (the second layer in Tables 1 and 2) thickness increased by 11–14% over $P/P_0 = 0.9$. The increase in the film thickness by propylene was almost the same as that by *n*-butane and was much lower than that by 1,3-butadiene. In particular, the film thickness increased by only 5.5% at $P/P_0 = 0.55$, over which the sudden increase in the permeability coefficient of propylene was observed. The increase in the permeability coefficient is probably due to the adsorption of propylene on the polyimide surface rather than swelling of the film. Of course, a lot of work will be required for understanding the sudden increase in the propylene permeability coefficient.

In conclusion, in propylene, we observed the surface layer on polyimide at $P/P_0 > 0.55$. The layer was thought to be the vapor adsorption layer of propylene. Moreover, the permeability of propylene rapidly increased at $P/P_0 > 0.6$. This may be due to the surface adsorption of propylene rather than the swelling of the film by propylene. We thought that the surface adsorption layer played an important role in explaining the hydrocarbon permeation phenomenon, because a permeation mechanism of hydrocarbon

Table 1
Best fitting calculation parameters of 6FDA-BAAF(1) in propylene using the double layer model. Double layer model with a surface layer on 6FDA-BAAF film (roughness σ_s: surface, σ_{12}: first layer/second layer, σ_b: second layer/substrate)

P/P_0	First layer				Second layer		
	σ_s (nm)	Density (g/cm^3)	Thickness (nm)	σ_{12} (nm)	Density (g/cm^3)	Thickness (nm)	σ_b (nm)
0.00	0.7 ± 0.1	–	–	–	1.41 ± 0.07	66.8 ± 0.2	0.9 ± 0.2
0.55	0.7 ± 0.3	0.8 ± 0.3	2.6 ± 0.5	1.2 ± 0.5	1.44 ± 0.08	70.5 ± 0.3	0.4 ± 0.2
0.68	0.7 ± 0.2	0.7 ± 0.3	3.2 ± 0.3	1.4 ± 0.4	1.43 ± 0.09	71.9 ± 0.3	0.5 ± 0.2
0.81	0.8 ± 0.2	0.8 ± 0.2	4.0 ± 0.4	1.0 ± 0.4	1.40 ± 0.13	74.3 ± 0.5	0.5 ± 0.4
0.96	1.1 ± 0.2	0.83 ± 0.10	5.8 ± 0.2	0.9 ± 0.2	1.41 ± 0.09	76.2 ± 0.3	0.6 ± 0.2

Table 2
Best fitting calculation parameters of 6FDA-BAAF(2) in propylene using double layer model. Double layer model; with a surface layer on 6FDA-BAAF film (roughness σ_s: surface, σ_{12}: first layer/second layer, σ_b: second layer/substrate)

P/P_0	First layer				Second layer		
	σ_s (nm)	Density (g/cm^3)	Thickness (nm)	σ_{12} (nm)	Density (g/cm^3)	Thickness (nm)	σ_b (nm)
0.00	0.5 ± 0.2	–	–	–	1.45 ± 0.06	30.7 ± 0.2	1.0 ± 0.2
0.72	0.9 ± 0.2	0.9 ± 0.2	3.8 ± 0.4	0.9 ± 0.4	1.38 ± 0.12	32.5 ± 0.3	0.5 ± 0.2
0.81	0.8 ± 0.2	0.7 ± 0.2	4.0 ± 0.4	1.4 ± 0.4	1.41 ± 0.10	33.2 ± 0.4	0.5 ± 0.5
0.99	0.9 ± 0.2	0.82 ± 0.11	5.5 ± 0.2	0.7 ± 0.3	1.38 ± 0.12	34.2 ± 0.3	0.5 ± 0.2

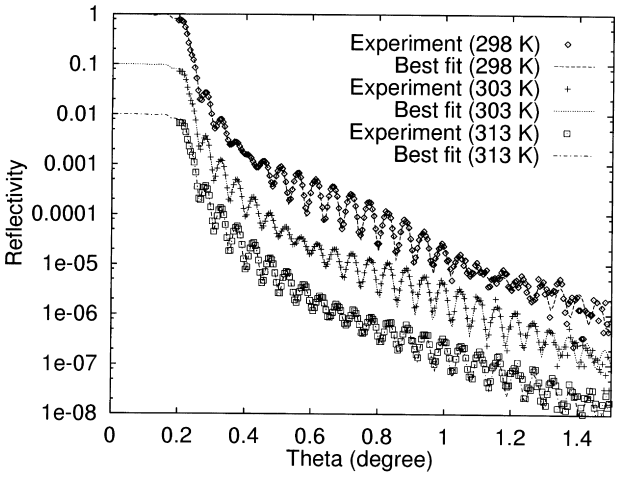

Fig. 6. X-ray reflectivities of 6FDA-BAAF(1) film in propylene (P/P_0 = 0.96) at 298 K (Experiment: ◇, Calculation: — —), at 303 K (Experiment: +, Calculation:- - -) and at 313 K (Experiment: □, Calculation: – ·–·–·).

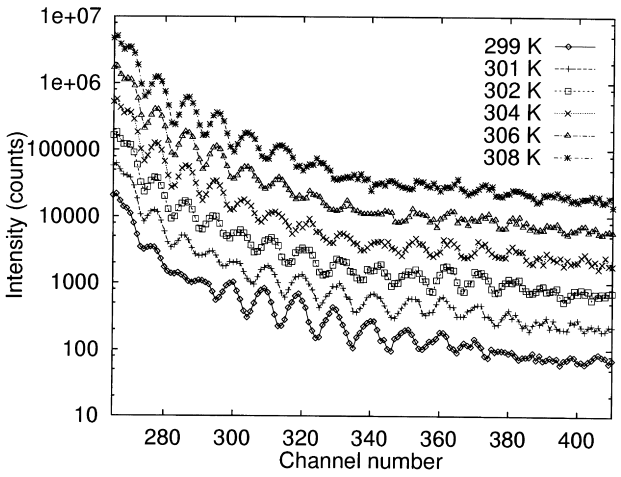

Fig. 7. X-ray reflectivities of 6FDA-BAAF(2) film in propylene (P/P_0 = 0.99) at 299 K (Experiment: ◇), at 301 K (Experiment: +), at 302 K (Experiment: □), at 304 K (Experiment: ×), at 306 K (Experiment: △) and at 308 K (Experiment: ∗).

gases different from that of the ideal gas applied to non-organic gas separation systems should be considered.

Further studies will be anticipated concerning the surface layer on polyimide. We have now studied the surface adsorption layer of propane and propane/propylene mixed gas on polyimide. In particular, the contents of propane and propylene in the surface layer of the mixed gas are thought to play an important role in gas selectivity. We plan the determination of the contents of propane and propylene in the surface layer using the labeling technique of neutron reflectivity measurement. This communication is the first report in these studies on the surface hydrocarbon gas adsorption layer on polyimide.

Acknowledgements

A part of this work was conducted with the support of the Petroleum Energy Center (PEC) subsidized by the Ministry of International Trade and Industry.

References

[1] Hachisuka H, Ohara T, Ikeda K. J Membr Sci 1996;116:265.
[2] R. Lee KR, Hwang ST. J Membr Sci 1992;73:37.
[3] Shimazu A, Hachisuka H, Ikeda K. Kagakukougaku 1995;60:262 (in Japanese).
[4] Okamoto K, Noborio K, Hao J, Tanaka K, Kita H. J Membr Sci 1997;134:171.
[5] Shimazu A, Miyazaki T, Maeda M, Matsushita M, Ikeda K. J Polym Sci, Polym Phys Ed 1999;37:2941.
[6] Shimazu A. Submitted for publication.
[7] Miyazaki T, Shimazu A, Matsushita T, Ikeda K. Submitted for publication.
[8] Russell TP. Mater Sci Rep 1990;5:171.
[9] Stamm M. Adv Polym Sci 1992;100:358.
[10] Toney MF, Tompson C. J Chem Phys 1989;92:3781.
[11] Toney MF, Brennan S. J Appl Phys 1989;66:1861.
[12] Lucas CA, Nguyen TD, Kortright JB. Appl Phys Lett 1991;59:2100.
[13] Beck tan NC, Wu WL, Wallace WE, Davis GT. J Polym Sci, Polym Phys Ed 1998;36:155.
[14] Parratt LG. Phys Rev 1954;95:359.
[15] Nevot L, Croce P. Rev Phys Appl 1980;15:761.
[16] Tadros ME, Hu P, Adamson AW. J Colloid Interface Sci 1974;49:184.
[17] Hu P, Adamson AW. J Colloid Interface Sci 1977;59:605.
[18] Lee WY, Slutsky LJ. J Phys Chem 1982;86:842.
[19] Beaglehole D. Phys Rev Lett 1987;58:1434.
[20] Gee ML, Healy TW, White LR. J Colloid Interface Sci 1989;131:18.
[21] Tidswell IM, Rabedeau TA, Pershan PS, Kosowsky SD. Phys Rev Lett 1991;66:2108.
[22] Beaglehole D, Radlinska EZ, Ninham BW, Christenson HK. Phys Rev Lett 1991;66:2084.
[23] Beaglehole D, Radlinska EZ, Ninham BW, Christenson HK. Langmuir 1991;7:1843.
[24] Beaglehole D, Christenson HK. J Phys Chem 1992;96:3395.